Journal of Hazardous Materials 454 (2023) 131447

Contents lists available at ScienceDirect

Journal of Hazardous Materials

journal homepage: www.elsevier.com/locate/jhazmat

The decomposition and emission factors of a wide range of PFAS in diverse, contaminated organic waste fractions undergoing dry pyrolysis

Erlend Sørmo [a,b,*], Gabriela Castro [c], Michel Hubert [a,d], Viktória Licul-Kucera [e,f], Marjorie Quintanilla [c], Alexandros G. Asimakopoulos [c], Gerard Cornelissen [a,b], Hans Peter H. Arp [a,c]

[a] Geotechnics and Environment, Norwegian Geotechnical Institute (NGI), Oslo, Norway
[b] Faculty of Environmental Sciences and Natural Resource Management, Norwegian University of Life Sciences (NMBU), Ås, Norway
[c] Department of Chemistry, Norwegian University of Science and Technology (NTNU), Trondheim, Norway
[d] Faculty of Engineering, Norwegian University of Science and Technology (NTNU), Trondheim, Norway
[e] Institute for Analytical Research, Hochschulen Fresenius gem. Trägesellschaft mbH, Idstein, Germany
[f] Institute for Biodiversity and Ecosystem Dynamics, University of Amsterdam, Amsterdam, Netherlands

HIGHLIGHTS

- A robust protocol for determination of PFAS in complex matrices such as sewage sludge and biochar.
- Multiple PFAS congeners present at elevated concentrations in eight different organic waste fractions.
- Residual PFAS concentrations in biochars produced between 500 and 800°C.
- > 95% of PFAS decomposed or accumulated in pyrolysis oil following dry pyrolysis > 500°C.
- Emission factors of PFAS during pyrolysis dominated by short chains and range 0.01 – 3.1 mg tonne^{-1}.

GRAPHICAL ABSTRACT

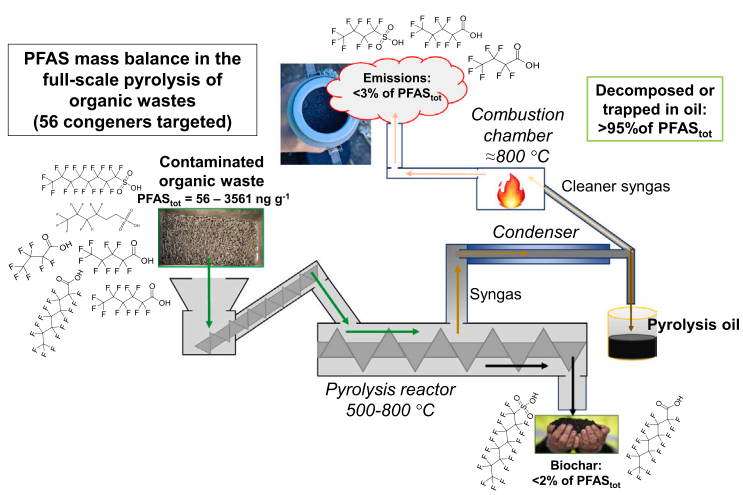

ARTICLE INFO

Editor: Feng Xiao

Keywords:
Pyrolysis
Sewage sludge
Organic waste

ABSTRACT

Current treatment options for organic waste contaminated with per- and polyfluoroalkyl substances (PFAS) are generally limited to incineration, composting or landfilling, all resulting in emissions. Dry pyrolysis is a promising emerging alternative to these practices, but there is uncertainty related to the fate of PFAS during this process. The present work first developed a robust method for the determination of PFAS in complex matrices, such as sewage sludge and biochar. Then, a mass balance was established for 56 different PFAS during full-scale pyrolysis (2–10 kg biochar hr^{-1}, 500–800 °C) of sewage sludges, food waste reject, garden waste and waste

* Corresponding author at: Geotechnics and Environment, Norwegian Geotechnical Institute (NGI), Oslo, Norway.
E-mail address: erlend.sormo@ngi.no (E. Sørmo).

https://doi.org/10.1016/j.jhazmat.2023.131447
Received 4 January 2023; Received in revised form 23 March 2023; Accepted 17 April 2023
Available online 18 April 2023
0304-3894/© 2023 The Author(s). Published by Elsevier B.V. This is an open access article under the CC BY license (http://creativecommons.org/licenses/by/4.0/).

PFAS
Biochar
Method development
Emission factors
Mass balance

timber. PFAS were found in all wastes (56–3651 ng g^{-1}), but pyrolysis resulted in a ≥ 96.9% removal. Residual PFAS (0.1–3.4 ng g^{-1}) were detected in biochars obtained at temperatures up to 750 °C and were dominated by long chain PFAS. Emitted PFAS loads ranged from 0.01 to 3.1 mg $tonne^{-1}$ of biochar produced and were dominated by short chain PFAS. Emissions made up < 3% of total PFAS-mass in the wastes. Remaining uncertainties are mainly related to the presence of thermal degradation products in flue gas and condensation oils.

1. Introduction

Per- and polyfluoroalkyl substances (PFAS) are a large group of synthetic organic chemicals used in an ever-widening range of industrial and consumer applications since the 1940 s [25]. Their spreading in the environment has led to adverse health effects, particularly endocrine disruption and carcinogenicity [56]. The strong carbon-fluorine bonds confer them high thermal stability, persistence and relatively high water solubility, which have made them ubiquitous in the environment [1,32] Particularly, compounds such as perfluoroalkyloctanoic acid (PFOA) and perfluoroalkyloctanoic sulfonate (PFOS) have been included in the Stockholm Convention [60,61], and thus, their production has shifted from long chain (CF_2 ≥7, where CF_2 represents the number of perfluorinated alkyls in a chain) towards short chain (6 ≤CF_2 ≥4) and ultrashort chain (3 ≤CF_2 ≥1) PFAS compounds [11,18]. The high mobility of short chain and ultrashort chain PFAS makes them spread fast in the environment and challenging to remove, e.g., in wastewater treatment plants (WWTPs), leading to a widespread occurrence in drink water sources [42]. Lately, attention has also been given to PFAS precursor compounds, such as perfluorooctylsulfonamides (FSA) and fluorotelomer alcohols, due to both the discovery of their toxicity and their environmental transformation pathways [74].

Due to their widespread use and environmental presence, PFAS compounds find their way into most waste streams, including municipal solid waste [8], electronic waste [57], sewage sludge [23,52,62,68], animal manure [40], food waste [43], composite wood building materials and textile waste [14]. Inadequate treatment of such waste streams has led to PFAS compounds being spread in the environment [34,52], and also presents a major challenge for recycling in the circular economy [27].

Modern waste incineration, usually operated at > 1000 ºC, has been an accepted approach to handling hazardous waste in many regions [16, 22], as modern waste incinerators readily degrade most organic contaminants and are designed with flue gas scrubbing and energy recovery. The fate of PFAS during waste incineration processes is not well understood and there are both concerns about unmonitored compounds, such as precursors, and ultrashort chain PFAS, and environmental risks related to the release of thermal degradation products [55]. During the last few decades, pyrolysis has received increased attention from the scientific community as a more sustainable thermal handling option for organic waste [15,35,36,66]. Pyrolysis entails heating up organic waste in absence of oxygen to produce syngas, oil and biochar [13]. Biochar is a porous carbon-rich product, with a versatile set of characteristics that can be exploited for multiple usages, such as agricultural soil improvement [29,31,45], carbon capture and storage [50], sorbents for organic contaminants [2,6,28], fillers in concrete [26], and substitutes for anthracite coal in metallurgical industry [70]. Furthermore, the effect of pyrolysis as a thermal treatment option to decompose organic contaminants has been demonstrated for pharmaceuticals, polychlorinated biphenyls (PCBs), polyaromatic hydrocarbons (PAHs) and endocrine disrupting and hormonal compounds [39], chlorophenols and chlorinated pesticides [53], as well as organophosphorus flame retardants [19].

Recently, Alinezhad et al. [7] demonstrated for soils that the type of thermal treatment, incineration or pyrolysis, does not matter in terms of PFAS removal as long as temperature and residence time are sufficient, i.e. > 500 °C and > 30 min, respectively. Other laboratory studies [64,69] have documented the degradation of a wide range of PFAS compounds, in spent activated carbon (AC) or in aqueous film forming foam (AFFF) respectively, under an inert atmosphere and similar conditions, and were able to detect a range of perfluoroalkene-, perfluoroalkane-, perfluoroalkyl aldehyde- and fluorotelomer alcohol degradation products. Nonetheless, they were not able to detect the specific ozone-harming perfluoroalkanes, perfluoromethane and perfluoroethane, or other short chain polyfluoroalkane greenhouse gases. McNamara et al. [38] furthermore documented that PFAS that don't degrade fully can accumulate in the pyrolysis oils during biosolids pyrolysis. These results are promising for pyrolysis as a waste handling alternative for PFAS-contaminated organic waste. However, as Stoiber et al. [55] noted in the case of waste incineration, the effects demonstrated in idealized laboratory studies might not be the same for full scale operations. Such a discrepancy has previously been documented in data from sewage sludge pyrolysis in two commercially operated plants that showed the presence of PFAS in flue gas scrubber water [58], although at low concentrations (PFOA at 13.2 ng L^{-1} and PFOSA at 46.2 ng L^{-1}). This suggests, to some extent, that PFAS compounds can survive a sequence of high temperature pyrolysis and combustion treatments in an upscaled system.

Hence, the purpose of the present study was to fill knowledge gaps related to the fate of PFAS during real-world, industrial pyrolysis of contaminated organic waste by exploring how feedstock and pyrolysis conditions affect the presence of PFAS in both biochar and the emitted exhaust from a medium scale pyrolysis system (operational up to 5–10 kg hr^{-1}). This was performed by testing the following hypotheses: 1) Given a high enough pyrolysis temperature, PFAS will be removed from the solid phase (feedstock to biochar) regardless of initial concentrations and composition of congeners and 2) a pyrolysis mass balance that includes emission factors will demonstrate that the majority of quantifiable PFAS compounds are decomposed in the process. This study presents the first investigation of PFAS in pyrolysis of organic waste types other than sewage sludge. To the best of the authors' knowledge, it is also the first to quantify the potential release of PFAS compounds from a medium scale pyrolysis system, let alone provided emission factors for PFAS from pyrolysis. This study also considered 56 different compounds, including ultrashort chain PFAS and PFAS precursors, which required the development of a novel and robust method for PFAS analysis in complex matrices such as sewage sludge and biochar.

2. Materials and methods

2.1. Chemicals and materials

PFAS standards were acquired from various providers or self-synthesized (see Table S1 for full details). Isotopically labelled internal standards: PFOA-$^{13}C_8$ (99%), PFOS-$^{13}C_8$ (99%) and 6:2 FTS-$^{13}C_2$-D_4 were bought from Cambridge Isotope Laboratories.

LC-MS grade Methanol (MeOH) and acetonitrile (ACN) were purchased from Merck (Darmstadt, Germany). Ethyl acetate (EtOAc, ≥99.7% v/v), ammonium acetate (≥98% w/w) and formic acid (FA, 96%) were supplied by VWR Chemicals (Trondheim, Norway). Ammonium acetate (>99% w/w) was bought from Fluka (Munich, Germany). Water was purified with a Milli-Q grade water system (Q-option, Elga Labwater, Veolia Water Systems LTD, U.K.) or purchased (LiChrosol®, UHPLC-MS grade) from Merck (Darmstadt, Germany). Whatman® Glass fiber filters (GFF) and Amberlite® XAD-2® was purchased from Merck (Darmstadt, Germany). Nitrogen (N_2, ≥99.6%) was acquired from Linde

Gas AS (Oslo, Norway).

2.2. Contaminated organic waste fractions

2.2.1. Waste fraction descriptions

Seven contaminated waste materials, and one reference material, were investigated in this study (Table 1). The waste materials included four sludges from wastewater treatment plants, one reject from food waste biogas production, and three wood-based fractions – waste timber, garden waste and wood chip pellets from forestry/logging. Based on existing literature, the waste fractions investigated were all expected to contain different concentrations of PFAS. The raw waste samples will be referred to as feedstocks for the pyrolysis process for the remainder of this study.

2.2.2. Bulk sampling and pre-treatment before pyrolysis

Samples of about 2 m^3 were collected in bulk at a randomly chosen time point for each feedstock by the respective waste handling companies/wastewater treatment plants. The relatively large sample size was based on the need to have both sufficient feedstock for the planned pyrolysis treatments and to assure representativeness. The full-size bulk samples were dried (moisture content 5–10%) using a batch paddle drier (1.5 ×5 m) made by Scanship AS (Tønsberg, Norway). The drier heats the sample material to about 102–110 °C by channelling superheated steam from a heat exchanger into a heating jacket fitted around the drier. The dried feedstocks were then pelletised (length 40 mm, radius 8 mm). Both pre-treatments, drying and pelletisation, were applied to homogenize the chemical composition and physical properties of the feedstocks before pyrolysis.

2.3. Pyrolysis

2.3.1. Pyrolysis technology

A medium scale Biogreen® pyrolysis unit (2–10 kg biochar hr^{-1}) built by ETIA Ecotechnologies (now a part of VOW ASA, Lysaker) was used in the present study (Figure S.1). In this unit, feedstock material was fed through a feeding screw with a vacuum lock, into the pyrolysis reactor which contains an electrically heated screw, the Spirajoule©, with a maximum temperature of 900 ºC. The feedstock material was converted to biochar as it moved along the screw, and residence time in the reactor was controlled by the rotational frequency of the screw. The reactor was operated at negative pressure to allow pyrolysis gas to be quickly separated from the biochar, as to minimize contact time between biochar and gas. The pyrolysis gas was channelled directly into a condenser unit where the gas was cooled to approximately 10 ºC. Pyrolysis oil was collected through a liquid lock while the syngas continued into a burner where it was combusted with propane at 800–900 ºC before being released as exhaust through a chimney.

2.3.2. Operational conditions

Feedstock feeding rates of 5–10 kg hr^{-1} were used. The wood-based substrates (wood chips, waste timber and garden waste) were run at around 5 kg hr^{-1}, to avoid tar-clogging between reactor and the condenser, while some of the sludge-based materials were processed at rates closer to 10 kg hr^{-1}. To remove O_2 from the system, the reactor and connecting pipes were flushed with N_2 for 10 min before the start. Residence time in the reactor was 20 min for all samples except for the de-watered sewage sludge, for which a 40 min residence time was used. The change in residence time for this feedstock only, was the result of a need to address technical challenges related to clogging of the feeder screw.

Pyrolysis temperature was considered the main treatment variable in this study, and the samples were pyrolyzed at two or more temperatures between 500 and 800 ºC (see Table 1 for details). Not all feedstocks were pyrolyzed at the same set of temperatures due to a combination of logistical and technical challenges. Treatment temperature was defined as measured in the biochar leaving the reactor at the end of the heated screw. After the pyrolysis set point temperature was reached, the reactor was run for another 1–2 hrs in order to reach stable conditions before sampling.

Gas emission measurements and sampling of biochar were done only during the period of stable conditions, which lasted approximately 2 hrs for each treatment temperature.

Biochar yield ($Y_{Biochar}$, %) at a specific treatment temperature was determined as the rate of biochar produced ($R_{biochar}$, kg hr^{-1}) divided by the feedstock feeding rate ($R_{feedstock}$, kg hr^{-1}) over the period defined as stable conditions:

$$Y_{Biochar} \quad (\%) = \frac{R_{Biochar}(kg \quad hr^{-1})}{R_{Feedstock}(kg \quad hr^{-1})} \times 100 \tag{1}$$

As a control, yield was also calculated for each step in the pyrolysis process (heating, stabilization, and cooling), and the sum of these respective yields were compared to the yield calculated by total feedstock in and total biochar out for the entire pyrolysis run.

Table 1
Description of the waste material feedstocks studied, conditions for their respective pyrolysis treatments, and sampling information.

Feedstock	Abbrev.	Description	Pyrolysis temperatures (ºC)	Pyrolysis residence time (min)	Solid phases sampled	Flue gas sampled
Digested sewage sludge	DSS-1	Sewage sludge and food waste gone through thermal hydrolysis (170 ºC) before anaerobic digestion for biogas production	500, 600, 700 and 750	20	Yes	Yes (excl. 750 ºC)
Digested sewage sludge	DSS-2	Sewage sludge gone through anaerobic digestion for biogas production	500, 600, 700 and 800	20	Yes	Yes
Limed sewage sludge	LSS	Sewage sludge gone through anaerobic digestion for biogas production, then added lime (39%) for stabilization/hygenization	600 and 750	20	Yes	Yes
Dewatered sewage sludge	DWSS	Raw sewage sludge, thermally hydrolysed (170 °C) and then dewatered using a heated centrifuge (100 °C).	600, 700 and 800	40	Yes	No
Reject from food waste biogas production	FWR	Fraction of food waste rejected from biogas production. Consists of material that does not pass an initial sieving process to reject plastics and other too large or non-digestible items.	600 and 800	20	Yes	No
Waste timber	WT	Discarded wood products and objects from private households, businesses, and construction/demolition (no chemically impregnated wood)	500, 600, 700 and 800	20	Yes	No
Garden waste	GW	Gardening waste from private households and businesses. Fraction includes twigs, leaves, roots, and some sand/gravel.	500, 600 and 800	20	Yes	No
Wood chips	CWC	Pellets produced from pine wood chips from forestry/logging.	500, 600, 700 and 750	20	Yes	No

2.4. Sampling and emission measurements

2.4.1. Solids sampling

Feedstock subsamples for chemical characterization were taken by random grab sampling (10–20 scoops, 1 kg) during the pelletisation process. Biochar subsamples were composed by random grab sampling (10–20 scoops, 1 kg) from the total amount of biochar (2–10 kg) produced during each treatment temperature. Both feedstock and biochar subsamples were air dried in the laboratory, crushed (D< 1 mm, controlled by sieve) and homogenized using a ball mill (Retsch ISO 9001) at 50 rpm for 10 min. Between each sample, the ball mill was scrubbed with soap, rinsed twice with MeOH:MilliQ (50%) and dried (100 ºC, 10 min).

Pyrolysis oil was collected in bulk through a liquid lock throughout the period of stable conditions. The bulk sample was split into an aqueous and an oil phase using a phase separating funnel. The fractions were weighed to establish the ratio between oil and water, before subsamples were collected by vigorously shaking and then pouring out the relative amounts of each phase to produce a smaller (100 mL) sample in HDPE bottles.

2.4.2. Gas emission sampling

Exhaust gas and aerosols were sampled from inside the chimney (the only exit for flue gas), within the inner 2/3 of the chimney diameter at about 20 cm below the outlet. Gas measurements were done for all the sewage sludge-based feedstocks, except for the DWSS (all treatments) and the DSS-1 (750 ºC treatment).

Particle based and gas phase contaminants in the exhaust were sampled using a low volume air sampler (Comde-Derenda, Stahnsdorf, Germany), operated at a rate of 2.4 m^3h^{-1}, that draws flue gas from the chimney into a cartridge with a GFF filter for aerosol collection (0.45 μm, pre-cleaned by heating to 450 °C for 8 hrs) followed by an XAD-2 sorbent for gas phase contaminants (dried at 105 °C for 24 hrs and pre-cleaned through Soxhlet-extraction with MeOH, ACN, toluene (8 hrs per solvent) and cyclohexane 4 hrs, ≈ 100 mL per sampling). A single point sample integrated over a period of 60 min was collected for each treatment temperature. The filter cartridge was rinsed with MeOH between each sampling. The combination of GFF and XAD-2 in a low volume air sampler has previously been used successfully in ambient air sampling of PFAS [12].

Carbon based gas composition of the exhaust – carbon monoxide (CO), carbon dioxide (CO_2), methane (CH_4), and non-methane volatile organic carbon [NMVOC = ethane (C_2H_6) + propane (C_3H_8) + ethylene (C_2H_4) + hexane (C_6H_{14}) + formaldehyde (CHOH)], in addition to hydrofluoric acid (HF), was determined using a portable Fourier Transform Infrared Spectrometer (FTIR) from Gasmet. One data point was recorded every three minutes (n ≈ 40 per treatment). Nitrogen (N_2) content in the sample was corrected for by running a N_2 blank before every sampling. Aerosol concentrations (≤10 μm, PM_{10}) were measured separately every 10–20 min (n = 6–12) with a pdr-1500 instrument from Thermo Scientific. PM_{10} concentrations were converted to total suspended particles (TSP) using a factor 1.4, as according to Sparrevik et al. [54]. Gas composition data was used to establish a carbon balance for the process (see Section 2.5).

2.5. Sample preparation and instrumental analysis

2.5.1. Carbon analysis

Total carbon in the feedstock and biochar samples was analysed in triplicates using the dry combustion method as described by Nelson & Sommers [41] with IR on a Leco CHN628 instrument. Total carbon in the pyrolysis oil condensates were determined through conversion of all carbon species to CO_2 through combustion with subsequent infrared detection according to method ASTM D5291 by Karlshammerverket Laboratory, Karlshamn, Sweden.

2.5.2. PFAS analysis

For the PFAS analysis two different extraction methods were used (extraction method A and B), and three different instrumental methods (instrumental method A, B and C). Extraction method A was combined with instrumental method A to target 41 congeners (method AA), while extraction method B was combined first with instrumental method B to target 11 congeners (method BB) and then with instrumental method C to target further 4 congeners (BC). Each method is summarized in short here, but full details can be found in SI, section C.

Extraction method A: This approach required method development, see the SI for details (section B). All feedstock, biochar, XAD and GFF samples were extracted for analysis, in triplicate, targeting 41 congeners that included 15 perfluorinatedalkylcarboxylic acids (PFCA), 9 perfluorinatedalkylsulphonic acids (PFSA), 4 fluorotelomere sulphonates (FTS), 8 fluorosulphonamides (FSA), and 5 miscellaneous substitute compounds. See the full list of congeners in the SI (Section A, and Table S1).

The extraction procedure used was based on Asimakopoulos et al. [10] with minor modifications: Ultrasound assisted extraction (UAE) was performed on 0.1 g sample in EtOAc (3 mL), ammonium acetate aqueous buffer and ultrasonication (45 min, 40 °C) followed by centrifugation (10 min, 4000 rpm). The UAE was repeated another two consecutive times to produce a final volume of ~9 mL (3 x 3 mL). Extract clean-up with 2 mL Milli-Q water and centrifugation (10 min, 4000 rpm) was undertaken before concentration under a gentle nitrogen stream (N_2, 35 ºC) to near dryness, and reconstitution in MeOH:Milli-Q (1 mL, 50:50).

Instrumental method A: The instrumental method used was based on Trimmel et al. [59] with minor modifications**.** Target analytes were determined with UPLC-MS/MS with a Xevo TQ-S triple quadrupole mass spectrometer, equipped with a Z spray ESI source, connected to an Acquity UPLC I-Class system, both acquired from Waters (Milford, MA, U.S.). Analytes were separated using a Kinetex C_{18} column (30 ×2.1 mm, 1.3 μm) serially connected to a C_{18} security guard (2 ×2.1 mm i.d.), both supplied by Phenomenex (Torrance, CA, U.S.).

Extraction method B: Two sewage sludge-based feedstocks (DSS-1 and DSS-2), their resulting biochars and the XAD-resins from gas emission measurements at all treatment temperatures were selected for quantification of additional PFAS. Due to limited sample amounts, GFF samples were not available for these analyses.

The samples were extracted following the protocol suggested by Ahmadireskety et al. [3] with modifications: UAE was applied on 0.2 g with NH_3/MeOH (1%, 5 mL) and ultrasonication (30 min, 40 °C), followed by centrifugation (10 min, 4000 rpm) and supernatant collection, repeated to produce a final supernatant volume of 10 mL. The supernatant was reduced until near dryness (N_2, 35 °C), before being reconstituted in MeOH (1 mL). An additional clean-up procedure was done by adding the supernatant sample (1 mL) to a mixture of acetic acid (100 μL, anhydrous) and Superclean™ ENVI-Carb™ (50 ± 5 mg). Vigorous shaking (30 s) and centrifugation (10 min, 4000 rpm) of the mixture was followed by supernatant collection and evaporation until near dryness (N_2, 35 °C), before reconstitution in ACN:Milli-Q (95:5) and filtration (recycled cellulose syringe filter, 0.2 μm).

Instrumental method B: This method was used to monitor 11 precursor compounds not included in method A, namely 7 perfluorinated alkanoic acids, 2 perfluoroalkoxy acetic acids and 2 perfluoroalkyl bisphosphates, see the SI for full details (section A, Table S1). They were analysed using reversed-phase liquid chromatography-mass spectrometry (RPLC-MS) on a Nexera XR HPLC system hyphenated to an Sciex QTrap 5500 System. Chromatographic separation was achieved using an XSelect HSS T3 column (50 ×2.1 mm, 3.5 μm) equipped with the corresponding pre-column (5 ×2.1 mm, 3.5 μm) held at 30 °C.

Instrumental method C: Ultrashort chain PFAS, 4 congeners, including 3 PFCA and 1 PFSA (see SI section A and Table S1) were analysed using hydrophilic interaction chromatography coupled to mass spectrometry (HILIC-MS), as previously described by Neuwald et al.

[42].

Instrumental methods B and C: For the ultrashort chain and additional precursor PFAS in this study no internal standards (or comparable internal standards) were available. Therefore, the actual samples were spiked before extraction and after extraction to evaluate absolute recoveries. The results can be found in Table S4.

2.6. Quality control and assurance

Procedural blanks were analysed to evaluate background contamination arising from the lab materials and solvents. During analysis, solvent blanks, and a standard solution were injected at regular intervals to check for any potential cross contamination or sample carryover, and to evaluate signal variations and drift. The injection needle was washed with a solution of MeOH:Milli-Q (50:50; v/v) with 0.1% FA before and after each injection.

To ensure accuracy and precision, multiple-point calibration curves were prepared: Instrumental method A: 11 points from 0.01 to 50 ng mL^{-1} in MeOH:Milli-Q (50:50, v/v), Instrumental method B: 7 points from 0.05 to 20 ng mL^{-1} in ACN:Milli-Q (95:5, v/v), and Instrumental method C: 7 points from 0.01 to 5 ng mL^{-1} was prepared in ACN: Milli-Q (95:5, v/v), demonstrating regression coefficients for all the studied compounds, $R^2 > 0.98$, $R^2 > 0.99$ and $R^2 > 0.999$, respectively. Two MS/MS transitions were optimized per TA. The most intense transition (higher S/N ratio) was considered as the quantification transition (1) and the second as the confirmation transition (2) (Table S2). The instrumental limits of quantification (iLOQs) were calculated for each target analyte as ten times the signal from the baseline noise (S/N ratio) and ranged from 0.01 to 5.00 ng mL^{-1} (Table S2). The method LOQs (mLOQs) were estimated accordingly with pre-extraction spiked samples and ranged from 0.25 to 50 ng mL^{-1} (Table S2). All samples were analysed in either duplicates (GFF) or triplicates (feedstocks, biochar and XAD) to control for sample heterogeneity and method error. Glass fiber filter samples were analysed in duplicates rather than triplicates due to limited amounts of sample material availability.

Obtained absolute recoveries (Abs%), relative recoveries (Rel%) and matrix effects (ME%) are presented in Table S4. Quantification of the target analytes was accomplished based on the internal standard method and matrix-matched calibration standards [48].

2.7. Data analysis

All concentrations are presented as ng g^{-1} dry weight (d.w.). For statistical analyses the numeric values of 0 and LOQ/2 were used in cases where one or two of the replicate data points were < LOD or LOQ respectively.

To estimate the relative effectiveness of pyrolysis as a waste treatment option for PFAS, the removal efficiency (RE) was calculated according to the equation suggested by Moško et al. [39]:

$$RE(\%) = 100\% - \left(\frac{C_{biochar} \times Y_{biochar}}{C_{feedstock}} \right) \quad (2)$$

where $C_{biochar}$ is the concentration (ng g^{-1}) in a biochar produced at a given pyrolysis temperature, $C_{feedstock}$ is the concentration (ng g^{-1}) in the feedstock and $Y_{biochar}$ is the yield (Eq. 1) of the biochar in the pyrolysis process. To avoid overestimation of RE, the discrete values of LOD and LOQ were used as $C_{biochar}$ for all compounds that were originally detected in the feedstock ($C_{feedstock}$ > LOD) but not in the resulting biochar.

Emission factors in mg $PFAS_{tot}$ per tonne of biochar produced (EF_{PFAS}, μg $tonne^{-1}_{biochar}$) were calculated using the carbon balance approach [21,47,54,72]. This method uses the carbon balance between feedstock going into the process and biochar, pyrolysis oil and flue gas coming out to calculate the net molar component-to-CO_2 emission ratios and thus the volume of flue gas produced ($V_{flue\ gas}$) (for details see SI, Section C). A measured concentration of PFAS in the flue gas ($conc_{PFAS}$) can thus be combined with the estimated $V_{flue\ gas}$ to yield the EF_{PFAS} (Eq. 3)

$$EF_{PFAS} = conc_{PFAS} \times V_{flue\ \ gas} \quad (3)$$

A mass balance for PFAS upon the pyrolysis of 1 tonne of each feedstock is set up based on total concentrations of PFAS in the feedstock and resulting biochar (adjusted by biochar yield) and emission factors for total PFAS. Only feedstocks and treatments for which biochar and emission data was available were included in the analysis (Table 1). No data on PFAS in the pyrolysis oil condensed from the syngas was acquired, since the extraction of PFAS from this matrix entailed analytical challenges that would not ensure the quality of the results; pyrolysis oil is a strongly acidic mixture of water, organic acids, phenols, alcohols, and complex high molecular mass organic compounds [46]. The fraction not found in biochar or exhaust is therefore considered to be either decomposed or in the pyrolysis oil.

3. Results and discussion

3.1. PFAS in feedstocks

In total, 26 out of the 41 PFAS-congeners analysed for using method AA were detected across the eight feedstocks (see Fig. 1, Table S.5), in concentrations ranging from 56–3651 ng g^{-1}. In addition, using method BB for two of the sewage sludge feedstocks (DSS-1 and DSS-2), 3 of the 11 additional precursor compounds were detected, but no ultrashort chain PFAS were detected (method BC). The sewage sludge feedstocks presented the largest variety of PFAS congeners: 9, 12, 10 and 9 different PFAS-congeners were detected in DSS-1, DSS-2, LSS, and DWSS respectively (Fig. 2). Eight congeners were detected in the food waste reject. Few congeners were detected in the wood-based feedstocks (five in WT, two in GW and five in CWC).

Sewage sludge feedstocks. The total amounts of PFAS ($PFAS_{tot}$) in the sewage sludge feedstocks were 56 ± 11, 441 ± 33, 340 ± 43 and 214 ± 88 ng g^{-1} for the DSS-1, DSS-2, LSS and DWSS respectively. These concentrations are similar to previously reported findings from around the globe [23,51,52,67]. The distribution of PFAS in the sewage sludge feedstocks (Fig. 1), DSS-1, DSS-2, LSS and DWSS, were mainly dominated by PFPeA (0, 76.3, 63.8. and 0% of $PFAS_{tot}$ respectively), followed by PFOS (25.4%, 8.6%, 3.8% and 16.2% of $PFAS_{tot}$ respectively) and 4:2 FTS (43.7%, 6.2%, 18.8% and 37.3% of $PFAS_{tot}$ respectively). Additionally, PFBA constituted 40% of the $PFAS_{tot}$ in the DWSS, but was not detected in the other sludge feedstock samples.

Wood-based feedstocks. PFAS in the wood-based feedstocks (114 – 3651 ng g^{-1}), wood chips (CWC), waste timber (WT) and garden waste (GW), were dominated by PFHxA (Fig. 1). This congener is a surfactant typically found in high concentrations in AFFF [5,18,30], but also in textiles [49], fluoropolymer production [63], wood composite building materials [14], vegetation from contaminated soils [24], and is furthermore the end product of natural oxidative degradation processes of precursor compounds [4]. The high concentration in the CWC (3651 ± 1846 ng g^{-1}), confirmed by a triplicate sample) could be a result of contamination during the production chain of the wood chip pellets.

Food waste reject feedstock. The second highest $PFAS_{tot}$ feedstock concentration was found in the food waste reject (FWR, 676 ± 62 ng g^{-1}), which was dominated by PFBA (32.3% of $PFAS_{tot}$), PFPeA (31.8% of $PFAS_{tot}$) and 4:2 FTS (33.0% of $PFAS_{tot}$). PFBA and PFPeA have previously been detected in packaging materials and non-stick ware connected to food processing and packaging [30,71]. These short chain congeners can furthermore stem from the food itself [24].

On the whole, the large concentration range (56–3651 ng g^{-1} $PFAS_{tot}$) and wide variety of PFAS-congeners (28 congeners) (Fig. 1) make the selected feedstocks well suited to demonstrate the effect of pyrolysis as a waste handling method for PFAS-contaminated organic waste, as the effect of thermal degradation of PFAS depends both upon total concentration and PFAS-type [7].

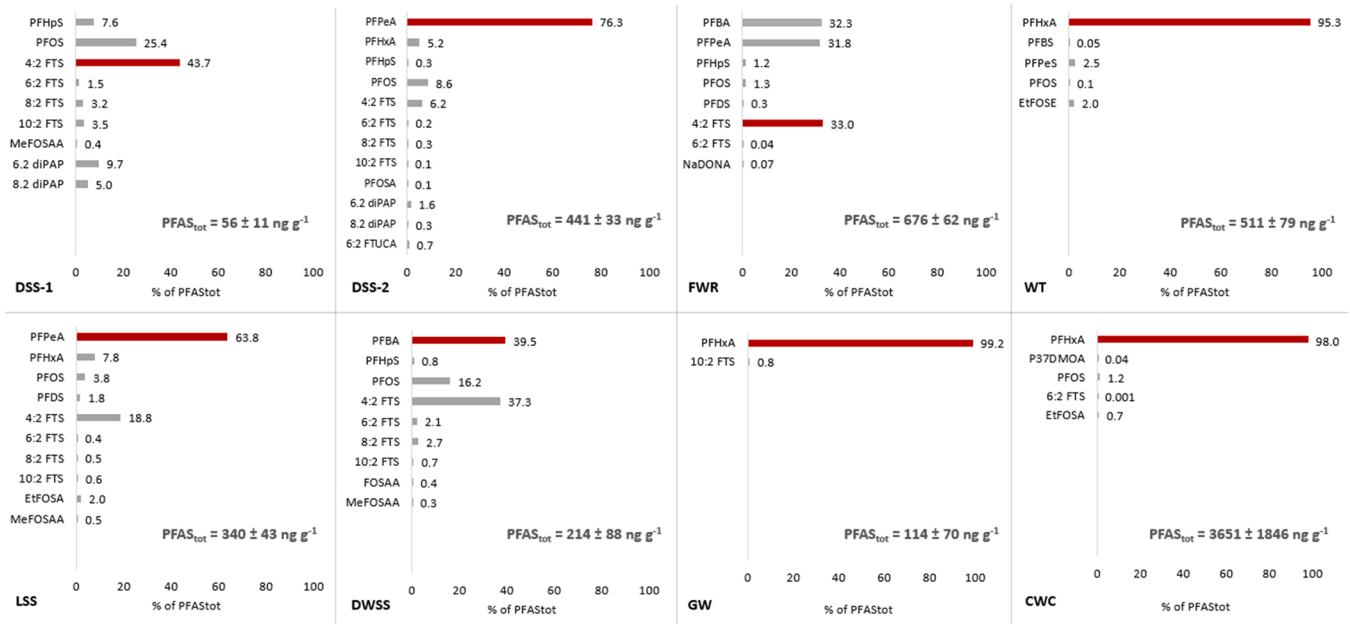

Fig. 1. Total concentration ($PFAS_{tot}$ ng g^{-1}) and distribution (% of $PFAS_{tot}$) of PFAS compounds detected in the digested sewage sludge (DSS-1 and DSS-2), limed sewage sludge (LSS), de-watered sewage sludge (DWSS), food waste reject (FWR), waste timber (WT), garden waste (GW), and wood chips (CWC) prior to pyrolysis treatment.

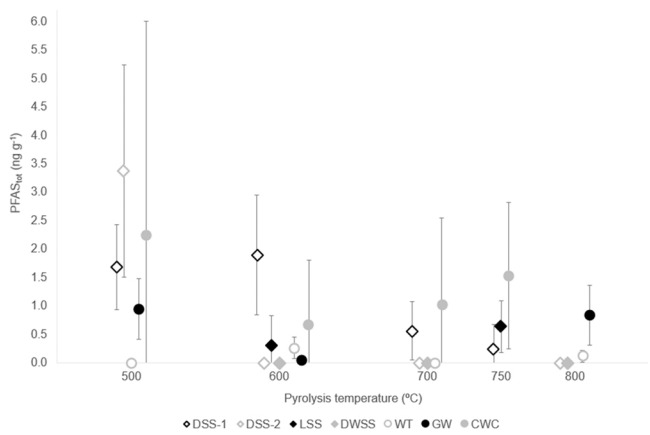

Fig. 2. Total PFAS ($PFAS_{tot}$, ng g^{-1}) in biochars produced at various pyrolysis temperatures (500–800 °C) from the digested sewage sludge (DSS-1 and DSS-2), limed sewage sludge (LSS), de-watered sewage sludge (DWSS), food waste reject (FWR), waste timber (WT), garden waste (GW), and wood chips (CWC). Data points and error bars are showing the mean and standard deviations from triplicate analysis.

3.2. PFAS in biochars

Concentrations of $PFAS_{tot}$ in the biochar samples ranged between <LOD and 3.4 ng g^{-1} (Fig. 2, Table S.5) and were thus 1–3 orders of magnitude less than the concentrations in the original feedstocks (details about removal efficiency in Section 3.3, Table 2). There was no statistically significant ($p > 0.05$) linear reduction in PFAS concentration with pyrolysis temperature. However, biochars produced at 500 °C had the highest $PFAS_{tot}$ concentrations (1 – 3.4 ng g^{-1}), except for WT biochar where no PFAS was detected (Table S.5). Meanwhile, no PFAS were detected in biochars produced at 800 °C. To the best of our knowledge, attempts to detect residual PFAS concentrations in biochar have previously only been made in pilot studies by Thoma et al. [58] and Kundu et al. [33]. In the former, PFAS in sewage sludge (biosolids) and resulting biochars from two commercial pyrolysis plants run at around 600 °C were investigated. They reported PFOS and PFOA (0.5 and 0.2 ng g^{-1} respectively), at concentrations 10 times lower than what was found in the present work. In the latter, sewage sludge was pyrolyzed at 500 and 600 °C to in a semi pilot scale unit, but the biochars produced had non-detectable concentrations (LODs not provided). In both studies however, little or no details were provided about the analytical methods used.

Table 2
Removal efficiency (RE, %) of $PFAS_{tot}$ in the transformation of digested sewage sludge (DSS-1 and DSS-2), limed sewage sludge (LSS), de-watered sewage sludge (DWSS), food waste reject (FWR), waste timber (WT), garden waste (GW), and wood chips (CWC) to biochars at various pyrolysis temperatures (500–800 °C).

Feedstock	Pyrolysis temp (°C)	RE (%)	Feedstock	Pyrolysis temp (°C)	RE (%)
DSS-1	500	> 96.93	FWR	600	> 99.95
	600	> 96.89		800	> 99.96
	700	> 98.18	WT	500	> 99.99
	750	> 98.35		600	> 99.98
DSS-2	500	> 99.55		700	> 99.99
	600	> 99.88		800	> 99.99
	700	> 99.87	GW	500	> 99.67
	800	> 99.99		600	> 99.95
LSS	600	> 99.92		800	> 99.81
	750	> 99.87	CWC	500	> 99.99
DWSS	600	> 99.92		600	> 99.99
	700	> 99.92		700	> 99.99
	800	> 99.93		750	> 99.99

Pyrolysis reduced the variety of PFAS congeners – the biochar samples contained 60–100% fewer congeners than their feedstock materials (Tables S.5). Alinezhad et al. [7] found that polyfluorinated compounds, such as FTS and FSA are more easily degraded than PFCA and PFSA, with the PFSAs being the most recalcitrant. The present study could indicate similar trends, as PFSAs and PFCAs made up the majority of PFAS (80%) detected in biochars (PFPeA, PFHxA, PFOA, PFNA, PFHpS, PFOS and P37DMOA), although trace amounts of 6:2 FTS (0.04–0.14 ng g^{-1}) were found in some of the WT (600 °C), GW (500 and 600 °C) and CWC (500, 600 and 700 °C) biochars, and 6:2 FTUCA (0.4 ± 0.2 in ng g^{-1}) was detected in DSS-2 at 500 °C (Table S.5). However, the presence of PFSAs

and PFCAs in the biochars could also be explained by thermal transformation of precursor compounds [65]. While short chain PFAS (≤6 CF_2-moieties) dominated PFAS presence in feedstock samples (Fig. 1; median fraction of short chain PFAS was 95% across the eight feedstocks (Table S.5)) a shift towards long chain PFAS (>6 CF_2-moieties) was observed for the biochars. Across all biochars in which PFAS were detected, the median fraction of long chain PFAS was 99% (Table S.5). No ultrashort chain PFAS compounds were detected in the biochars. This biochar PFAS-fingerprint could be explained by long chain PFAS having a higher thermal stability and would hence be corroborated by Xiao et al. [64], who observed a decreasing thermal stability of PFCAs with decreasing tail length when studying the regeneration of spent activated carbon through thermal decomposition. Another reason for the dominance of long chain PFAS in the biochars could be that short chain PFAS are more easily evaporated to the gas phase. This argument is supported by both the high presence of short chain species in the flue gas (see Section 3.4) and by Blotevogel et al. [17], who did not see any chain length dependence on thermal stability in a mathematical modelling study of PFAS incineration.

3.3. PFAS Removal Efficiencies

Removal efficiencies (RE) for $PFAS_{tot}$ were larger than 96.9% (Table 2) across all treatment temperatures (500–800 °C) and feedstocks (sludge and wood based). Note that RE (Eq. 2) is corrected by biochar yield to consider mass reduction (2–5 times original mass, Table S.6) during the pyrolysis process. The lowest REs were recorded for DSS-1 at 500 °C and 600 °C (96.93% and 96.89%, respectively). At treatment temperatures ≥ 700 °C however, more than 98% of $PFAS_{tot}$ was removed from all feedstocks. These results are in agreement with Alinezhad et al. [7] who presented the decomposition of PFAS in soil under thermal treatments, demonstrating that RE after pyrolysis at 500 °C and residence time of 30 min was above 99%, regardless of PFAS initial load and type. In the present study, the residence time applied in the pyrolysis experiments was 20 min. It could be possible that by increasing the residence time, higher RE% would have been obtained.

The somewhat lower RE recorded for DSS-1 compared to the other feedstocks is probably due to the DSS-1 feedstock having a relatively larger amount of the long chain sulfonate, PFOS (14 ng g^{-1}, 25.4% of $PFAS_{tot}$), which is likely less volatile or more recalcitrant towards thermal degradation [7] than the PFAS congeners that dominated some of the other feedstocks (see Section 3.2 for more details).

Overall, the temperatures required to achieve REs > 98% for PFAS being higher than 700 °C is similar to or higher than reported for other organic contaminants as Moško et al. [39] demonstrated for pharmaceuticals, PCBs, PAHs and endocrine disrupting and hormonal compounds, in sewage sludge pyrolysis. For organophosphate flame retardants (OPFRs), as documented in a parallel study by our group using the same samples [19], pyrolysis temperatures ≥ 500 °C were sufficient to achieve REs ~100%. The relative persistence to thermal degradation of PFAS compared to other organic contaminants is however expected, due to the high energy of the C-F bond relative to that of C-C and C-Cl bonds [44]. Nonetheless, an important caveat to these results is that several non-target PFAS (i.e. PFAS other than the 56 analysed for) may have been produced, such as per and polyfluorinated alkanes and alkenes with and without a head group [7,69].

3.4. PFAS Emission Factors

PFAS were detected in the flue gas (post syngas combustion) from the pyrolysis of the sewage sludge feedstocks at all treatment temperatures (Table 3), demonstrating that pyrolysis at ≥ 500 °C coupled with syngas combustion at 800–900 °C does not fully decompose PFAS present in the original feedstock. This is corroborated by Thoma et al. [58] who detected PFAS in flue gas scrubber water of pyrolysis units run at 600 °C with syngas combustion at 1020 °C. Total PFAS-concentrations in the exhaust, both particle and gaseous fractions included, ranged from <LOD to 100 ng m^{-3} with a mean concentration of 50 ± 70 ng m^{-3}. The mean concentration of gaseous PFAS (40 ± 61 ng m^{-3}) was somewhat higher than the particle based PFAS (10 ± 11 ng m^{-3}), but samples from both fractions demonstrated high heterogeneity (large standard deviations). Mathematical modelling has demonstrated that similar temperatures as applied in the present study (700–900 °C) should be sufficient to degrade PFAS [9,17]. The present findings of remaining PFAS after syngas combustion are probably representative for many after-combustion units. Our findings thus indicate that extra consideration needs to be put into designing a suitable combustion chamber for full-scale pyrolysis units allowing for sufficient residence time and gas

Table 3
Emission concentrations (ng m^{-3}) for PFAS detected in flue gas from the pyrolysis of digested sewage sludge (DSS-1 and DSS-2) and limed sewage sludge (LSS), along with the relative fractions of total PFAS found in the gaseous and particle-based fractions (%). Emission factors (EF, mg $tonne^{-1}$) for total PFAS also shown. Concentrations and EF shown as mean ± standard deviation.

Metric	PFAS type	PFAS compound	DSS-1			DSS-2				LSS	
			500	600	700	500	600	700	800	600	750
Emission concentrations (ng m^{-3})	PFCA	PFBA	n.d.	10.76 ± 0.02	11.5 ± 0.4	n.d.	3.6 ± 0.2	7.4 ± 0.5	9 ± 1	9.4 ± 0.5	12 ± 2
		PFPeA	2.0 ± 0.4	26 ± 36	n.d.	n.d.	9 ± 15	n.d.	n.d.	n.d.	n.d.
		PFHpA	n.d.	100 ± 99	35 ± 61	n.d.	n.d.	n.d.	n.d.	n.d.	n.d.
		7 H-PFHpA	n.d.	22 ± 27	n.d.	n.d.	n.d.	n.d.	n.d.	n.d.	n.d.
	PFSA	PFBS	42 ± 10	58 ± 16	46 ± 6	n.d.	n.d.	n.d.	10.9 ± 0.8	0.19 ± 0.03	n.d.
			n.d.	n.d.	n.d.	0.6 ± 0.8	n.d.	n.d.	n.d.	n.d.	n.d.
	FTS	6:2 FTS	n.d.	n.d.	0.03 ± 0.05	n.d.	n.d.	n.d.	n.d.	n.d.	n.d.
		8:2 FTS	n.d.	n.d.	n.d.	n.d.	8 ± 14	n.d.	n.d.	n.d.	n.d.
	FSA	PFOSA	n.d.	n.d.	n.d.	n.d.	6 ± 11	n.d.	n.d.	n.d.	n.d.
		MeFOSAA	11 ± 19	n.d.	n.d.	n.d.	n.d.	n.d.	n.d.	n.d.	n.d.
	Misc.	NaDONA	5 ± 9	n.d.	3 ± 6	n.d.	n.d.	n.d.	n.d.	n.d.	n.d.
	Sum	$PFAS_{tot}$	**59** ± 23	**217** ± 110	**96** ± 62	**0.6** ± 0.8	**27** ± 23	**7.4** ± 0.5	**20** ± 1	**9.6** ± 0.5	**12** ± 2
	Sum	Gaseous (%)	97	94	88	0	87	0	55	0	0
		Particles (%)	**3**	**6**	**12**	**100**	**13**	**100**	**45**	**100**	**100**
EF (mg $tonne^{-1}$)	Sum	$PFAS_{tot}$	0.2 ± 0.1	3.1 ± 1.6	1.2 ± 0.8	0.01 ± 0.02	0.9 ± 0.8	0.32 ± 0.02	0.7 ± 0.1	0.0096 ± 0.0005	0.9 ± 0.2

mixing to achieve complete degradation.

Unlike the biochar samples, where long chain PFAS dominated (Tables S.5), short chain PFAS represented the majority (60%) of all PFAS detected in the exhaust, particle-bound, and gaseous fractions. The two carboxylic acids with 3 and 4 CF_2-moieties, PFBA and PFPeA, and the sulfonic acid with 4 CF_2-moieties, PFBS, comprised 44–100% of all PFAS detected in the exhaust, despite not being detected in the feedstock pyrolyzed. Yao et al. [69] suggested radical mediated chain scission either at the functional head or at random sites along the chain as the most probable thermal degradation pathway for PFAS. In our study ultrashort chain PFAS compounds were, however, not detected in the gaseous phase of the flue gas, and they were not analysed for in the particle phase due to practical difficulties. The dominance of short chain PFAS could therefore be the result of one or more of the following explanations: short chain PFAS more easily evaporating to the flue gas (M. [73], partial degradation of longer chain PFAS by chain scission [69], and/or conversion of precursor compounds to short chain PFSA and PFCA [65].

Calculated $EF_{PFAStot}$ (Eq. 7) show that a range of 0.01 – 3.1 mg of $PFAS_{tot}$ were emitted per tonne of biochar produced from the sewage sludges studied (Table 3). EF_{PFAS} for all single PFAS compounds detected are compiled in Table S.8 and the calculated volumes of syngas used to derive these factors are shown in Table S.9. To the authors' knowledge, EF_{PFAS} have never been reported, either for dry pyrolysis or full scale waste incineration plants [55]. Thus, there is no literature to compare the present results to. The EF_{PFAS} are about 10–1000 times lower than emission factors for polycyclic aromatic hydrocarbons (PAHs) from the pyrolysis of waste timber at 600 ºC, as previously documented by our group [53]. However, it is expected that PAH emissions should largely exceed PFAS emissions, as these compounds can be generated from carbon matrices during pyrolysis and combustion [37].

3.5. PFAS Mass Balance using pyrolysis as a waste treatment option

The potential of pyrolysis as a waste treatment alternative was assessed through the mass balance of total PFAS in the pyrolysis treatment of 1 tonne of feedstock (Table 4). Three feedstocks (DSS-1, DSS-2 and LSS) and the pyrolysis temperatures applied in their treatments (500 – 800 ºC) were considered. Of the total amount of PFAS present in the feedstocks, a small fraction ends up in the biochar (<2%) regardless of pyrolysis temperature and feedstock, as is also reflected by the calculated removal efficiencies (Table 2). However, regarding emissions themselves, a similarly small fraction is released with flue gas through the chimney (<3%). This means that the large majority of PFAS (>95%) in the feedstocks is either decomposed in the pyrolysis reactor or combustion chamber, trapped in the pyrolysis oil, and/or released as degradation products not targeted in the present work. Possible future work could consist of total Extractable Organic Fluorine (EOF) non-target analyses of the biochar and pyrolysis oil to improve the organofluorine mass balance.

The mass balance varied somewhat with pyrolysis temperature, but it appeared that the factor that affects the distribution the most, is the composition of PFAS congeners in the feedstock. The sample DSS-1, with a relatively high concentration of PFOS (14 ± 4 ng g^{-1}), pyrolyzed at 600 °C can be considered as the worst-case scenario, for which 1.73% of $PFAS_{tot}$ would end up in the biochar, 2.81% would be emitted and 95.47% would be decomposed (Table 4). The best-case scenario on the other hand would be the pyrolysis of the DSS-2 feedstock, which has almost 10 times higher concentration in the feedstock than DSS-1, but which is dominated by short chain PFCAs and FTS (Fig. 2). Pyrolyzing the DSS-2 feedstock at 600 °C, would result in 0.00% ending up in the biochar, 0.08% being emitted and 99.92% being decomposed. Considering the fact that most options for handling PFAS-containing waste lead to some sort of emission, either through flue gas, landfill leachate or soil runoff [55], the relatively large amount that is decomposed using the pyrolysis approach could be worth the emissions caused, especially if emissions can be lowered, e.g. by optimizing the pyrolysis process for PFAS removal, or more simply by a filter solution.

As some of the feedstock and temperature treatment combinations yielded high particle-based emissions (up to 100%, Table 3) it is expected that emissions can be reduced by introducing a flue gas scrubber, an established technology for waste incineration. Wet scrubbers are especially efficient for scenarios when the target contaminants are associated with particles, as reported by [20] who demonstrated a reduction of 90% in emissions of dioxins from waste incinerators with high particle loads. Thoma et al. [58] did not quantify PFAS-emissions, but detected PFAS in water from wet scrubbing of exhaust during the pyrolysis of sewage sludge, thereby indicating scavenging of PFAS compounds from the flue gas. Thus, there is a need to properly document the effect of flue gas cleaning technology on PFAS-emissions from pyrolysis. It is also important to note that the present work accounts for emissions of a wide range of PFAS-congeners and precursor compounds, but has not documented the release of other possible thermal degradation products identified in laboratory studies, such as perfluoroalkanes, perfluoroalkenes, perfluoralkyl aldehydes and fluorotelomere alcohols [7,69]. The presence of said compounds in exhaust from commercial pyrolysis units could be challenging to document due to the need for advanced technology such as online gas chromatography systems. A first approach could therefore be to assess the environmental risk related to the emissions of potential degradation products identified in laboratory studies.

There is also a need to quantify PFAS in pyrolysis oil. This fraction contains both water and organic oily liquids, with the interface between those potentially acting as a scavenging phase for surface-active PFAS compounds. McNamara et al. [38] detected certain PFAS compounds, e.g. PFBA, in the pyrolysis oil at concentrations higher than in the feedstock, during laboratory scale pyrolysis of biosolids, suggesting that specific PFAS and their thermal conversion products can accumulate in this phase. This means that a significant amount of the fraction not accounted for in biochar or emitted gases in the present study could be in the pyrolysis oil. If this is indeed the case, the oil will have to be handled/used in such a way that further emissions will not occur. At the

Table 4
Mass balance for $PFAS_{tot}$ in the pyrolysis of 1 tonne of sewage sludge (DSS-1, DSS-2 and LSS) at temperatures between 500 and 800 °C.

In feedstock (1 tonne)		In biochar			Emitted		Decomposed or trapped in pyrolysis oil	
Sample	**$PFAS_{tot}$ (mg)**	**Pyr temp (ºC)**	**$PFAS_{tot}$ (mg)**	**$F_{biochar}$ (%)**	**$PFAS_{tot}$ (mg)**	**$F_{emitted}$ (%)**	**$PFAS_{tot}$ (mg)**	**$F_{decomposed}$ (%)**
DSS-1	55.6	500	0.91	1.64	0.13	0.231	54.6	98.13
		600	0.96	1.73	1.56	2.808	53.1	95.47
		700	0.30	0.55	0.67	1.203	54.6	98.25
DSS-2	429.4	500	1.36	0.32	0.01	0.001	428	99.68
		600	0.00	0.00	0.33	0.077	429.1	99.92
		700	0.00	0.00	0.12	0.029	429.3	99.97
		800	0.00	0.00	0.25	0.058	429.2	99.94
LSS	339.6	600	0.17	0.05	0.01	0.002	339.4	99.95
		750	0.29	0.09	0.41	0.12	338.9	99.79

local level, the pyrolysis oil and syngas could themselves be combusted as a heat source on site, including for the heating of the pyrolysis unit itself, which would further destroy the residual PFAS.

4. Conclusions

The present work has demonstrated that dry pyrolysis has potential as a waste handling alternative for PFAS-contaminated organic waste. For optimization towards PFAS removal, an adequately high pyrolysis temperature and residence time must be used. Considering the results from the present and previous studies, pyrolysis of contaminated organic waste should be operated at a minimum of 600 °C in order to properly decompose PFAS and other organic contaminants to non-detectable levels.

The nature of the feedstock and the type of PFAS present in the samples should also be considered, as removal efficiencies differed among the different feedstock pyrolyzed. Long chain PFAS accumulate to a larger extent in the biochar than short chain PFAS. Therefore, pyrolysis conditions should be adjusted to individual feedstocks, to achieve optimal removal of PFAS from the solid matrix.

The fraction of PFAS in the original organic wastes that ends up being released with the flue gas is relatively low (<3%). However, despite that the emissions make up a small fraction of the total mass of PFAS being treated, the total emissions from large-scale operations could be significant. Considering that the complete presence and nature of degradation products in the flue gas is unknown, flue gas cleaning might be necessary to avoid PFAS compounds being cycled back into the environment; alternatively, pyrolysis conditions and the pyrolysis reactor design could be optimized to either lower the formation of short chain PFAS, or to capture them quantitatively in the pyrolysis oil. Such optimization would require a better understanding of the organofluorine mass balance, that could be generated through total organofluorine analysis as well as non-target analysis.

PFAS decomposition seems to be a motivation for adopting dry pyrolysis as a waste handling option; however, future studies should consider other externalities, such as life cycle impacts compared to the status quo options of sending the contaminated feedstocks to incinerators, landfills, or to be used as fertilizer in agricultural areas.

Environmental implications

Dry pyrolysis has been suggested as a promising alternative for handling organic waste as it combines thermal destruction of contaminants, energy generation, and production of useful carbon-rich biochar for diverse applications. Such applications include soil quality improvement or soil amendment for contaminant risk abatement. There are, however, uncertainties related to the fate of organic contaminants in the pyrolysis process. The present study presents the decomposition and emission factors of a wide range of PFAS during the dry pyrolysis of diverse organic wastes in a full-scale unit (2–10 kg biochar hr^{-1}), thus providing important information for future assessments on the environmental impact of pyrolysis as a waste handling option.

CRediT authorship contribution statement

Erlend Sørmo – Funding acquisition, conceptualization, methodology, investigation, formal analysis, visualization, writing – original draft, writing – review & editing, Gabriela Castro – Supervision, methodology, investigation, formal analysis, validation, writing – review & editing, Michel Hubert – Investigation, formal analysis, writing – review & editing, Viktória Licul-Kucera – Investigation, formal analysis, writing – review & editing, Marjorie Quintanilla – Investigation, formal analysis, writing – review & editing, Alexandros G. Asimakopoulos – Supervision, resources, data curation, validation, writing – review & editing, Gerard Cornelissen – Supervision, project administration, funding acquisition, conceptualization, methodology, writing – review & editing, Hans Peter H. Arp – Supervision, project administration, funding acquisition, conceptualization, methodology, writing – review & editing.

Declaration of Competing Interest

The authors declare that they have no known competing financial interests or personal relationships that could have appeared to influence the work reported in this paper.

Data Availability

Data will be made available on request.

Acknowledgements

The authors acknowledge funding from the Research Council of Norway, through the joint-industry sustainability (BIA-X) project "Valorization of Organic Waste" (VOW) (NFR 299070) and the Miljøforsk project SLUDGEFFECT (NFR 302371); and from the European Union's Horizon 2020 research and innovation programme under the Marie Skłodowska-Curie Action grant agreement No 860665 (PERFORCE3 Innovative Training Network). Natalia Kasian, Gudny Flatabø, Hartantyo Seto Guntoro, Aadam Maczko and Bendik Bache Hansen from Scanship are acknowledged for assisting in biochar production, Caroline Berge Hansen, Gabrielle Dublet Adli and Maren Valestrand Tjønneland at NGI for contributing to field work and Irene E. Eriksen Dahl for biochar elemental analysis at NMBU. The PFAS analysis (method AA) was carried out in the EnviroChemistry Lab at NTNU, and at the Institute for Analytical Research, HSF (method BB and BC).

Appendix A. Supporting information

Supplementary data associated with this article can be found in the online version at doi:10.1016/j.jhazmat.2023.131447.

References

[1] Abunada, Z.-A., Alazaiza, M.Y.D., Bashir, M.J.K., 2020. I-an overview of per-and polyfluoroalkyl substances (PFAS) in the environment: source, fate, risk and regulations. Water 12 (12). https://doi.org/10.3390/w12123590.
[2] Ahmad, M., Rajapaksha, A.U., Lim, J.E., Zhang, M., Bolan, N., Mohan, D., et al., 2014. Biochar as a sorbent for contaminant management in soil and water: A review. Chemosphere 99, 19–33. https://doi.org/10.1016/j.chemosphere.2013.10.071.
[3] Ahmadireskety, A., Da Silva, B.F., Townsend, T.G., Yost, R.A., Solo-Gabriele, H.M., Bowden, J.A., 2021. Evaluation of extraction workflows for quantitative analysis of per- and polyfluoroalkyl substances: A case study using soil adjacent to a landfill. Sci Total Environ 760, 143944. https://doi.org/10.1016/j.scitotenv.2020.143944.
[4] Ahrens, L., Bundschuh, M., 2014. Fate and effects of poly- and perfluoroalkyl substances in the aquatic environment: A review. Environ Toxicol Chem 33 (9), 1921–1929. https://doi.org/10.1002/etc.2663.
[5] Ahrens, L., Norström, K., Viktor, T., Cousins, A.P., Josefsson, S., 2015. Stockholm Arlanda Airport as a source of per- and polyfluoroalkyl substances to water, sediment and fish. Chemosphere 129, 33–38. https://doi.org/10.1016/j.chemosphere.2014.03.136.
[6] Alhashimi, H.A., Aktas, C.B., 2017. Life cycle environmental and economic performance of biochar compared with activated carbon: A meta-analysis. Resour Conserv Recycl 118, 13–26. https://doi.org/10.1016/j.resconrec.2016.11.016.
[7] Alinezhad, A., Challa Sasi, P., Zhang, P., Yao, B., Kubátová, A., Golovko, S.A., et al., 2022. An investigation of thermal air degradation and pyrolysis of per- and polyfluoroalkyl substances and aqueous film-forming foams in soil. ACS EST Eng 2 (2), 198–209. https://doi.org/10.1021/acsestengg.1c00335.
[8] Allred, B.M., Lang, J.R., Barlaz, M.A., Field, J.A., 2015. Physical and biological release of poly- and perfluoroalkyl substances (PFASs) from municipal solid waste in anaerobic model landfill reactors. Environ Sci Technol 49 (13), 7648–7656. https://doi.org/10.1021/acs.est.5b01040.
[9] Altarawneh, M., Almatarneh, M.H., Dlugogorski, B.Z., 2022. Thermal decomposition of perfluorinated carboxylic acids: Kinetic model and theoretical requirements for PFAS incineration. Chemosphere 286, 131685. https://doi.org/10.1016/j.chemosphere.2021.131685.
[10] Asimakopoulos, A.G., Wang, L., Thomaidis, N.S., Kannan, K., 2014. A multi-class bioanalytical methodology for the determination of bisphenol A diglycidyl ethers, p-hydroxybenzoic acid esters, benzophenone-type ultraviolet filters, triclosan, and triclocarban in human urine by liquid chromatography–tandem mass

spectrometry. J Chromatogr A 1324, 141–148. https://doi.org/10.1016/j.chroma.2013.11.031.
[11] Ateia, M., Maroli, A., Tharayil, N., Karanfil, T., 2019. The overlooked short- and ultrashort-chain poly- and perfluorinated substances: A review. Chemosphere 220, 866–882. https://doi.org/10.1016/j.chemosphere.2018.12.186.
[12] Barber, J.L., Berger, U., Chaemfa, C., Huber, S., Jahnke, A., Temme, C., et al., 2007. Analysis of per- and polyfluorinated alkyl substances in air samples from Northwest Europe. J Environ Monit 9 (6), 530–541. https://doi.org/10.1039/B701417A.
[13] Barry, D., Barbiero, C., Briens, C., Berruti, F., 2019. Pyrolysis as an economical and ecological treatment option for municipal sewage sludge. Biomass Bioenergy 122, 472–480. https://doi.org/10.1016/j.biombioe.2019.01.041.
[14] Bečanová, J., Melymuk, L., Vojta, Š., Komprdová, K., Klánová, J., 2016. Screening for perfluoroalkyl acids in consumer products, building materials and wastes. Chemosphere 164, 322–329. https://doi.org/10.1016/j.chemosphere.2016.08.112.
[15] Beesley, L., Moreno-Jiménez, E., Gomez-Eyles, J.L., Harris, E., Robinson, B., Sizmur, T., 2011. A review of biochars' potential role in the remediation, revegetation and restoration of contaminated soils. Environ Pollut 159 (12), 3269–3282. https://doi.org/10.1016/j.envpol.2011.07.023.
[16] Block, C., Van Caneghem, J., Van Brecht, A., Wauters, G., Vandecasteele, C., 2015. Incineration of hazardous waste: a sustainable process. Waste Biomass Valoriz 6 (2), 137–145. https://doi.org/10.1007/s12649-014-9334-3.
[17] Blotevogel, J., Giraud, R.J., Rappé, A.K., 2023. Incinerability of PFOA and HFPO-DA: Mechanisms, kinetics, and thermal stability ranking. Chem Eng J 457, 141235. https://doi.org/10.1016/j.cej.2022.141235.
[18] Buck, R.C., Franklin, J., Berger, U., Conder, J.M., Cousins, I.T., de Voogt, P., et al., 2011. Perfluoroalkyl and polyfluoroalkyl substances in the environment: Terminology, classification, and origins. Integr Environ Assess Manag 7 (4), 513–541. https://doi.org/10.1002/ieam.258.
[19] Castro, G., Sørmo, E., Yu, G., Sait, S.T.L., González, S.V., Arp, H.P.H., et al., 2023. Analysis, occurrence and removal efficiencies of organophosphate flame retardants (OPFRs) in sludge undergoing anaerobic digestion followed by diverse thermal treatments. Sci Total Environ 870, 161856. https://doi.org/10.1016/j.scitotenv.2023.161856.
[20] Choi, K.-I., Lee, D.-H., 2007. PCDD/DF concentrations at the inlets and outlets of wet scrubbers in Korean waste incinerators. Chemosphere 66 (2), 370–376. https://doi.org/10.1016/j.chemosphere.2006.04.094.
[21] Cornelissen, G., Pandit, N.R., Taylor, P., Pandit, B.H., Sparrevik, M., Schmidt, H.P., 2016. Emissions and char quality of flame-curtain 'Kon Tiki' kilns for farmer-scale charcoal/biochar production. PLoS One 11 (5), e0154617. https://doi.org/10.1371/journal.pone.0154617.
[22] Dempsey, C.R., Oppelt, E.T., 1993. Incineration of hazardous waste: a critical review update. Air Waste 43 (1), 25–73. https://doi.org/10.1080/1073161X.1993.10467116.
[23] Gallen, C., Eaglesham, G., Drage, D., Nguyen, T.H., Mueller, J.F., 2018. A mass estimate of perfluoroalkyl substance (PFAS) release from Australian wastewater treatment plants. Chemosphere 208, 975–983. https://doi.org/10.1016/j.chemosphere.2018.06.024.
[24] Ghisi, R., Vamerali, T., Manzetti, S., 2019. Accumulation of perfluorinated alkyl substances (PFAS) in agricultural plants: A review. Environ Res 169, 326–341. https://doi.org/10.1016/j.envres.2018.10.023.
[25] Glüge, J., Scheringer, M., Cousins, I.T., DeWitt, J.C., Goldenman, G., Herzke, D., et al., 2020. An overview of the uses of per- and polyfluoroalkyl substances (PFAS). Environ Sci Process Impacts 22 (12), 2345–2373. https://doi.org/10.1039/D0EM00291G.
[26] Gupta, S., Kua, H.W., 2019. Carbonaceous micro-filler for cement: Effect of particle size and dosage of biochar on fresh and hardened properties of cement mortar. Sci Total Environ 662, 952–962. https://doi.org/10.1016/j.scitotenv.2019.01.269.
[27] Hale, S.E., Kalantzi, O.I., Arp, H.P.H., 2022. Introducing the EU project ZeroPM: zero pollution of persistent, mobile substances. Environ Sci Eur 34 (1), 108. https://doi.org/10.1186/s12302-022-00681-5.
[28] Hale, S.E., Arp, H.P.H., Kupryianchyk, D., Cornelissen, G., 2016. A synthesis of parameters related to the binding of neutral organic compounds to charcoal. Chemosphere 144, 65–74. https://doi.org/10.1016/j.chemosphere.2015.08.047.
[29] Hale, S.E., Nurida, N.L., Jubaedah, Mulder, J., Sørmo, E., Silvani, L., et al., 2020. The effect of biochar, lime and ash on maize yield in a long-term field trial in a Ultisol in the humid tropics. Sci Total Environ 719, 137455. https://doi.org/10.1016/j.scitotenv.2020.137455.
[30] Herzke, D., Olsson, E., Posner, S., 2012. Perfluoroalkyl and polyfluoroalkyl substances (PFASs) in consumer products in Norway – A pilot study. Chemosphere 88 (8), 980–987. https://doi.org/10.1016/j.chemosphere.2012.03.035.
[31] Ippolito, J.A., Spokas, K.A., Novak, J.M., Lentz, R.D., Cantrell, K.B., 2015. Biochar elemental composition and factors influencing nutrient retention. In *Biochar for Environmental Management: Science, Technology and Implementation*, 2nd ed. Routledge.
[32] Krafft, M.P., Riess, J.G., 2015. Per- and polyfluorinated substances (PFASs): Environmental challenges. Curr Opin Colloid Interface Sci 20 (3), 192–212. https://doi.org/10.1016/j.cocis.2015.07.004.
[33] Kundu, S., Patel, S., Halder, P., Patel, T., Hedayati Marzbali, M., Pramanik, B.K., et al., 2021. Removal of PFASs from biosolids using a semi-pilot scale pyrolysis reactor and the application of biosolids derived biochar for the removal of PFASs from contaminated water. Environ Sci Water Res Technol 7 (3), 638–649. https://doi.org/10.1039/D0EW00763C.
[34] Lang, J.R., Allred, B.M., Field, J.A., Levis, J.W., Barlaz, M.A., 2017. National estimate of per- and polyfluoroalkyl substance (PFAS) release to U.S. municipal landfill leachate. Environ Sci Technol 51 (4), 2197–2205. https://doi.org/10.1021/acs.est.6b05005.
[35] Lehmann, J., Gaunt, J., Rondon, M., 2006. Bio-char sequestration in terrestrial ecosystems – a review. Mitig Adapt Strateg Glob Change 11 (2), 403–427. https://doi.org/10.1007/s11027-005-9006-5.
[36] Li, L., Zou, D., Xiao, Z., Zeng, X., Zhang, L., Jiang, L., et al., 2019. Biochar as a sorbent for emerging contaminants enables improvements in waste management and sustainable resource use. J Clean Prod 210, 1324–1342. https://doi.org/10.1016/j.jclepro.2018.11.087.
[37] Mastral, A.M., Callén, M.S., 2000. A review on polycyclic aromatic hydrocarbon (PAH) emissions from energy generation. Environ Sci Technol 34 (15), 3051–3057. https://doi.org/10.1021/es001028d.
[38] McNamara, P., Samuel, M.S., Sathyamoorthy, S., Moss, L., Valtierra, D., Cortes Lopez, H., et al., 2023. Pyrolysis transports, and transforms, PFAS from biosolids to py-liquid. Environ Sci Water Res Technol 9 (2), 386–395. https://doi.org/10.1039/D2EW00677D.
[39] Moško, J., Pohořelý, M., Cajthaml, T., Jeremiáš, M., Robles-Aguilar, A.A., Skoblia, S., et al., 2021. Effect of pyrolysis temperature on removal of organic pollutants present in anaerobically stabilized sewage sludge. Chemosphere 265, 129082. https://doi.org/10.1016/j.chemosphere.2020.129082.
[40] Munoz, G., Michaud, A.M., Liu, M., Vo Duy, S., Montenach, D., Resseguier, C., et al., 2022. Target and nontarget screening of PFAS in biosolids, composts, and other organic waste products for land application in France. Environ Sci Technol 56 (10), 6056–6068. https://doi.org/10.1021/acs.est.1c03697.
[41] Nelson, D.W., Sommers, L.E. (1982). Total Carbon, Organic Carbon and Organic Matter. In A. L. Page, R. H. Miller, & D. R. Keeney (Eds.), Methods of soil analysis Part 2 Agronomy 9 (2nd ed., pp. 539–579). American Society of Agronomy.
[42] Neuwald, I.J., Hübner, D., Wiegand, H.L., Valkov, V., Borchers, U., Nödler, K., et al., 2022. Occurrence, distribution, and environmental behavior of persistent, mobile, and toxic (PMT) and very persistent and very mobile (vPvM) substances in the sources of german drinking water. Environ Sci Technol 56 (15), 10857–10867. https://doi.org/10.1021/acs.est.2c03659.
[43] O'Connor, J., Mickan, B.S., Siddique, K.H.M., Rinklebe, J., Kirkham, M.B., Bolan, N.S., 2022. Physical, chemical, and microbial contaminants in food waste management for soil application: a review. Environ Pollut 300, 118860. https://doi.org/10.1016/j.envpol.2022.118860.
[44] O'Hagan, D., 2008. Understanding organofluorine chemistry. An introduction to the C–F bond. Chem Soc Rev 37 (2), 308–319. https://doi.org/10.1039/B711844A.
[45] Obia, A., Mulder, J., Martinsen, V., Cornelissen, G., Børresen, T., 2016. In situ effects of biochar on aggregation, water retention and porosity in light-textured tropical soils. Soil Tillage Res 155, 35–44. https://doi.org/10.1016/j.still.2015.08.002.
[46] Papari, S., Hawboldt, K., 2018. A review on condensing system for biomass pyrolysis process. Fuel Process Technol 180, 1–13. https://doi.org/10.1016/j.fuproc.2018.08.001.
[47] Pennise, D.M., Smith, K.R., Kithinji, J.P., Rezende, M.E., Raad, T.J., Zhang, J., et al., 2001. Emissions of greenhouse gases and other airborne pollutants from charcoal making in Kenya and Brazil. J Geophys Res Atmos. 106 (D20), 24143–24155. https://doi.org/10.1029/2000JD000041.
[48] Raposo, F., Barceló, D., 2021. Challenges and strategies of matrix effects using chromatography-mass spectrometry: An overview from research versus regulatory viewpoints. TrAC Trends Anal Chem 134, 116068. https://doi.org/10.1016/j.trac.2020.116068.
[49] Rodgers, K.M., Swartz, C.H., Occhialini, J., Bassignani, P., McCurdy, M., Schaider, L.A., 2022. How well do product labels indicate the presence of PFAS in consumer items used by children and adolescents. Environ Sci Technol 56 (10), 6294–6304. https://doi.org/10.1021/acs.est.1c05175.
[50] Schmidt, H.-P., Anca-Couce, A., Hagemann, N., Werner, C., Gerten, D., Lucht, W., et al., 2019. Pyrogenic carbon capture and storage. GCB Bioenergy 11 (4), 573–591. https://doi.org/10.1111/gcbb.12553.
[51] Semerád, J., Hatasová, N., Grasserová, A., Černá, T., Filipová, A., Hanč, A., et al., 2020. Screening for 32 per- and polyfluoroalkyl substances (PFAS) including GenX in sludges from 43 WWTPs located in the Czech Republic—Evaluation of potential accumulation in vegetables after application of biosolids. Chemosphere 261, 128018. https://doi.org/10.1016/j.chemosphere.2020.128018.
[52] Sepulvado, J.G., Blaine, A.C., Hundal, L.S., Higgins, C.P., 2011. Occurrence and fate of perfluorochemicals in soil following the land application of municipal biosolids. Environ Sci Technol 45 (19), 8106–8112. https://doi.org/10.1021/es103903d.
[53] Sørmo, E., Silvani, L., Thune, G., Gerber, H., Schmidt, H.P., Smebye, A.B., et al., 2020. Waste timber pyrolysis in a medium-scale unit: Emission budgets and biochar quality. Sci Total Environ 718, 137335. https://doi.org/10.1016/j.scitotenv.2020.137335.
[54] Sparrevik, M., Adam, C., Martinsen, V., Jubaedah, Cornelissen, G., 2015. Emissions of gases and particles from charcoal/biochar production in rural areas using medium-sized traditional and improved "retort" kilns. Biomass Bioenergy 72, 65–73. https://doi.org/10.1016/j.biombioe.2014.11.016.
[55] Stoiber, T., Evans, S., Naidenko, O.V., 2020. Disposal of products and materials containing per- and polyfluoroalkyl substances (PFAS): A cyclical problem. Chemosphere 260, 127659. https://doi.org/10.1016/j.chemosphere.2020.127659.
[56] Sunderland, E.M., Hu, X.C., Dassuncao, C., Tokranov, A.K., Wagner, C.C., Allen, J. G., 2019. A review of the pathways of human exposure to poly- and perfluoroalkyl substances (PFASs) and present understanding of health effects. J Expo Sci Environ Epidemiol 29 (2), 131–147. https://doi.org/10.1038/s41370-018-0094-1.

[57] Tansel, B., 2022. PFAS use in electronic products and exposure risks during handling and processing of e-waste: A review. J Environ Manag 316, 115291. https://doi.org/10.1016/j.jenvman.2022.115291.
[58] Thoma, E.D., Wright, R.S., George, I., Krause, M., Presezzi, D., Villa, V., et al., 2022. Pyrolysis processing of PFAS-impacted biosolids, a pilot study. J Air Waste Manag Assoc 72 (4), 309–318. https://doi.org/10.1080/10962247.2021.2009935.
[59] Trimmel, S., Vike-Jonas, K., Gonzalez, S.V., Ciesielski, T.M., Lindstrøm, U., Jenssen, B.M., et al., 2021. Rapid determination of per- and polyfluoroalkyl substances (PFAS) in harbour porpoise liver tissue by HybridSPE®–UPLC®–MS/MS. Toxics 9 (8). https://doi.org/10.3390/toxics9080183.
[60] UNEP. (2017). Report of the Persistent Organic Pollutants Review Committee on the work of its thirteenth meeting.
[61] UNEP. (2019). Perfluorooctane sulfonic acid, its salts and perfluorooctane sulfonyl fluoride (SC-9/4).
[62] Venkatesan, A.K., Halden, R.U. (2013). National inventory of perfluoroalkyl substances in archived U.S. biosolids from the 2001 EPA National Sewage Sludge Survey. Journal of Hazardous Materials, 252–253, 413–418. https://doi.org/10.1016/j.jhazmat.2013.03.016.
[63] Wang, Z., Cousins, I.T., Scheringer, M., Buck, R.C., Hungerbühler, K., 2014. Global emission inventories for C4–C14 perfluoroalkyl carboxylic acid (PFCA) homologues from 1951 to 2030, part II: The remaining pieces of the puzzle. Environ Int 69, 166–176. https://doi.org/10.1016/j.envint.2014.04.006.
[64] Xiao, F., Sasi, P.C., Yao, B., Kubátová, A., Golovko, S.A., Golovko, M.Y., et al., 2020. Thermal stability and decomposition of perfluoroalkyl substances on spent granular activated carbon. Environ Sci Technol Lett 7 (5), 343–350. https://doi.org/10.1021/acs.estlett.0c00114.
[65] Xiao, F., Sasi, P.C., Alinezhad, A., Golovko, S.A., Golovko, M.Y., Spoto, A., 2021. Thermal decomposition of anionic, zwitterionic, and cationic polyfluoroalkyl substances in aqueous film-forming foams. Environ Sci Technol 55 (14), 9885–9894. https://doi.org/10.1021/acs.est.1c02125.
[66] Xiao, X., Chen, B., Chen, Z., Zhu, L., Schnoor, J.L., 2018. Insight into multiple and multilevel structures of biochars and their potential environmental applications: a critical review. Environ Sci Technol 52 (9), 5027–5047. https://doi.org/10.1021/acs.est.7b06487.
[67] Yan, H., Zhang, C.-J., Zhou, Q., Chen, L., Meng, X.-Z., 2012. Short- and long-chain perfluorinated acids in sewage sludge from Shanghai, China. Chemosphere 88 (11), 1300–1305. https://doi.org/10.1016/j.chemosphere.2012.03.105.
[68] Yang, G., Zhang, N., Yang, J., Fu, Q., Wang, Y., Wang, D., et al., 2020. Interaction between perfluorooctanoic acid and aerobic granular sludge. Water Res 169, 115249. https://doi.org/10.1016/j.watres.2019.115249.
[69] Yao, B., Sun, R., Alinezhad, A., Kubátová, A., Simcik, M.F., Guan, X., et al., 2022. J Hazard Mater 436, 129313. https://doi.org/10.1016/j.jhazmat.2022.129313. V.
[70] Ye, L., Peng, Z., Wang, L., Anzulevich, A., Bychkov, I., Kalganov, D., et al., 2019. Use of biochar for sustainable ferrous metallurgy. JOM 71 (11), 3931–3940. https://doi.org/10.1007/s11837-019-03766-4.
[71] Zafeiraki, E., Costopoulou, D., Vassiliadou, I., Bakeas, E., Leondiadis, L., 2014. Determination of perfluorinated compounds (PFCs) in various foodstuff packaging materials used in the Greek market. Chemosphere 94, 169–176. https://doi.org/10.1016/j.chemosphere.2013.09.092.
[72] Zhang, J., Smith, K.R., Ma, Y., Ye, S., Jiang, F., Qi, W., et al., 2000. Greenhouse gases and other airborne pollutants from household stoves in China: A database for emission factors. Atmos Environ 34 (26), 4537–4549. https://doi.org/10.1016/S1352-2310(99)00450-1.
[73] Zhang, M., Yamada, K., Bourguet, S., Guelfo, J., Suuberg, E.M., 2020. Vapor pressure of nine perfluoroalkyl substances (PFASs) determined using the knudsen effusion method. J Chem Eng Data 65 (5), 2332–2342. https://doi.org/10.1021/acs.jced.9b00922.
[74] Zhang, W., Pang, S., Lin, Z., Mishra, S., Bhatt, P., Chen, S., 2021. Biotransformation of perfluoroalkyl acid precursors from various environmental systems: Advances and perspectives. Environ Pollut 272, 115908. https://doi.org/10.1016/j.envpol.2020.115908.